



# Humulane-Type Macrocyclic Sesquiterpenoids From the Endophytic Fungus *Penicillium* sp. of *Carica papaya*

Fu-Run Wang<sup>1,2†</sup>, Li Yang<sup>1†</sup>, Fan-Dong Kong<sup>4†</sup>, Qing-Yun Ma<sup>1</sup>, Qing-Yi Xie<sup>1</sup>, You-Gen Wu<sup>2</sup>, Hao-Fu Dai<sup>5</sup>, Ping Chen<sup>2\*</sup>, Na Xiao<sup>3\*</sup> and You-Xing Zhao<sup>1\*</sup>

<sup>1</sup>Haikou Key Laboratory for Research and Utilization of Tropical Natural Products, Institute of Tropical Bioscience and Biotechnology, CATAS, Haikou, China, <sup>2</sup>Key Laboratory for Quality Regulation of Tropical Horticultural Crops of Hainan Province, College of Horticulture, Hainan University, Haikou, China, <sup>3</sup>State Key Laboratory of Crop Biology, College of Agronomy, Shandong Agriculture University, Tai'an, Shandong, China, <sup>4</sup>Key Laboratory of Chemistry and Engineering of Forest Products, State Ethnic Affairs Commission, Guangxi Key Laboratory of Chemistry and Engineering of Forest Products, Guangxi Collaborative Innovation Center for Chemistry and Engineering of Forest Products, School of Chemistry and Chemical Engineering, Guangxi University for Nationalities, Nanning, China, <sup>5</sup>Hainan Institute for Tropical Agricultural Resources, CATAS, Haikou, China

## OPEN ACCESS

### Edited by:

Xiachang Wang,  
Nanjing University of Chinese  
Medicine, China

### Reviewed by:

Weaam Ebrahim,  
Mansoura University, Egypt  
Sherif S. Ebada,  
Ain Shams University, Egypt  
Orazio Tagliatela-Scafati,  
University of Naples Federico II, Italy

### \*Correspondence:

Ping Chen  
chenping08213@163.com  
Na Xiao  
xiaona198707@126.com  
You-Xing Zhao  
zhaoyouxing@itbb.org.cn

<sup>†</sup>These authors have contributed  
equally to this work

### Specialty section:

This article was submitted to  
Organic Chemistry,  
a section of the journal  
Frontiers in Chemistry

Received: 19 October 2021

Accepted: 15 November 2021

Published: 16 December 2021

### Citation:

Wang F-R, Yang L, Kong F-D, Ma Q-Y,  
Xie Q-Y, Wu Y-G, Dai H-F, Chen P,  
Xiao N and Zhao Y-X (2021)  
Humulane-Type Macrocyclic  
Sesquiterpenoids From the  
Endophytic Fungus *Penicillium* sp. of  
*Carica papaya*.  
Front. Chem. 9:797858.  
doi: 10.3389/fchem.2021.797858

Three new humulane-type sesquiterpenoids, penirolide A (**1**), penirolide B (**2**), and 10-acetyl-phomanoxide (**3**), together with three known compounds aurasperone A (**4**), pughiiinin A (**5**), and cyclo(L-Leu-L-Phe) (**6**) were isolated from the endophytic fungus *Penicillium* sp. derived from the leaves of *Carica papaya* L. Their structures including their absolute configurations were determined based on the analysis of NMR and HRESIMS spectra, NMR chemical shifts, and ECD calculations. Compounds **2**, **3**, **5**, and **6** significantly inhibited glucagon-induced hepatic glucose production, with EC<sub>50</sub> values of 33.3, 36.1, 18.8, and 32.1 μM, respectively. Further study revealed that compounds **2**, **3**, **5**, and **6** inhibited hepatic glucose production by suppression of glucagon-induced cAMP accumulation.

**Keywords:** endophytic fungus, *Penicillium* sp., humulane-type sesquiterpenoid, anti-diabetic activity, cAMP accumulation

## INTRODUCTION

Endophytic fungi, living in plants but non-pathogenic, have been proven to be promising sources of secondary metabolites with unusual structures as well as intriguing pharmacology activities, and become interesting and important resources for drug discovery (Strobel, 2003; Uzma et al., 2018; Gupta et al., 2020; Zhang et al., 2006). In recent years, increasing attention has been attracted to metabolite profiles of endophytic fungi from medicinal plants (Kaul et al., 2012). Papaya, *Carica papaya* L. (papaya), an edible and medicinal plant cultivated in tropical and subtropical regions, has been used as topical dressings for ulcer and dermatitis treatment, has gastrointestinal uses such as anti-helminthic and antibacterial activity treatments, has been used as anti-arthritis treatment, and has traditional uses for fertility control (Krishna et al., 2008; Pinnamaneni, 2017).

In our continuing search for structurally novel and biologically active secondary metabolites from endophytic fungi, three new humulane-type sesquiterpenoids, penirolides A (**1**) and B (**2**), and 10-acetyl-phomanoxide (**3**), were isolated from the endophytic fungus *Penicillium* sp. derived from the leaves of papaya. Humulane-type sesquiterpenoids, an uncommon type of compounds featuring an 11-membered macrocycle, were found in plants, liverworts, and fungi, and exhibited various

bioactivities including antibacterial, antifungal, cytotoxic, and immunosuppressive activities (Liao et al., 2013; Luo et al., 2006; Toyota et al., 2004). Due to the flexible 11-membered macrocycle in the molecule, elucidation of the stereochemistry of humulane-type sesquiterpenoids is very challenging. Chiral derivatization and chemical conversions were successfully applied to clarify their configurations (Liao et al., 2013). However, limited amounts of sample available hampers broad use of these methods in the structural elucidation of natural products. Quantum calculations of NMR shifts represents a simple, useful, and fast alternative in address complex stereochemical problems by comparing experimental and computed values using parameters (Lodewyk et al., 2012; Grimblat and Sarotti, 2016), such as correlation coefficient, mean absolute error (MAE), corrected mean absolute error (CMAE), CP3 parameter (Smith and Goodman, 2009), DP4 probability (Smith and Goodman, 2010), or its improved version, DP4+ probability (Grimblat et al., 2015), avoiding chemical derivatization. In our effort to determine the configurations of the new humulane-type sesquiterpenoids (**1–3**), extensive spectroscopic analysis including 1D and 2D NMR spectra, NMR chemical shift calculations coupled with DP4+ probability analysis, and ECD calculations were utilized. In addition, all the isolates were evaluated for their anti-diabetic activity on a glucagon-induced glucose production model in mouse hepatocytes. Herein, the isolation, structural elucidation, and biological activities of compounds **1–6** **Figure 1** were reported.

## RESULTS AND DISCUSSION

Compound **1** was isolated as yellow oil. Its molecular formula was determined as  $C_{15}H_{26}O_4$  from the positive ion peak at  $m/z$  293.1723  $[M + Na]^+$  (calcd for  $C_{15}H_{26}NaO_4$ , 293.1723), requiring three indices of hydrogen deficiency. The  $^1H$  NMR spectrum (**Table 1**) showed signals for two olefinic protons ( $\delta_H$  5.47 and 5.43), three methylenes ( $\delta_H$  1.27–2.28), three oxygenated methines ( $\delta_H$  2.93, 3.43, and 3.44), and four methyls ( $\delta_H$  1.06, 1.08, 1.11, and 1.24). The  $^{13}C$  NMR spectrum revealed the presence of 15 carbons, which were classified by HSQC spectrum as one double bond ( $\delta_C$  122.8 and 144.7), three methylenes ( $\delta_C$  38.1, 45.1, and 45.6), three oxygenated methines ( $\delta_C$  75.6, 80.3, and 63.7), three quaternary carbons ( $\delta_C$  36.1, 67.1, and 75.6) including two oxygenated, and four methyls ( $\delta_C$  16.5, 22.3, 26.7, and 28.5). The  $^1H$ – $^1H$  COSY spectrum of **1** presented three coupling spin systems, H-7 $\alpha$ /H-7 $\beta$ –H-8, H-3 $\alpha$ /H-3 $\beta$ –H-4–H-5, and H-10–H-11 $\alpha$ /H-11 $\beta$ –H-1 (**Figure 2**). The HMBC correlations (**Figure 2**) from  $\underline{CH}_3$ -13 ( $\delta_H$  1.06, s)/ $\underline{CH}_3$ -14 (1.11, s) to C-5 ( $\delta_C$  144.7), C-6 ( $\delta_C$  36.1), and C-7 ( $\delta_C$  45.1), from H-7 $\alpha$  ( $\delta_H$  1.91, s)/H-7 $\beta$  ( $\delta_H$  1.27, s) to C-5, from  $\underline{CH}_3$ -12 (1.08, s) to C-1 ( $\delta_C$  80.3), C-2 ( $\delta_C$  75.6), and C-3 ( $\delta_C$  45.6), from H-3 $\alpha$  ( $\delta_H$  2.20, s)/H-3 $\beta$  ( $\delta_H$  2.28, s) to C-1, and from  $\underline{CH}_3$ -15 (1.24, s) to C-8 ( $\delta_C$  63.7), C-9 ( $\delta_C$  67.1), and C-10 ( $\delta_C$  75.6) connected the three coupling spin systems and formed the humulane-type sesquiterpenoid skeleton. The olefinic bond and the macrocycle accounted for two indices of hydrogen deficiency.

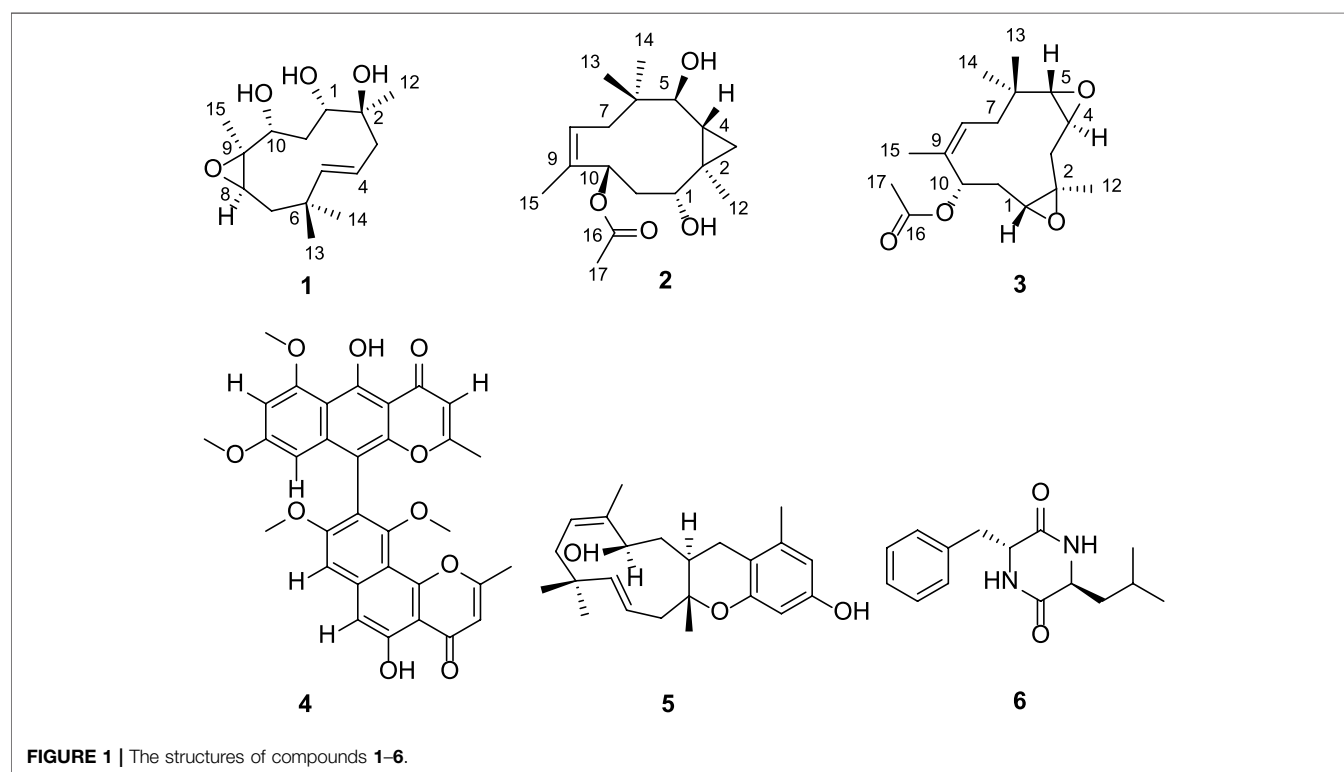
The remaining one degree of unsaturation together with the analysis of the chemical shift of C-8 and C-9 suggested the existence of oxirane ring at positions 8 and 9.

The vicinal coupling constant ( $J = 15.8$  Hz) between H-4 and H-5 assigned the *E* configured  $\Delta^4$  double bond. In the ROESY spectrum, the key correlation of  $\underline{CH}_3$ -15 with H-8 ( $\delta_H$  2.93) indicated that  $\underline{CH}_3$ -15 and H-8 were cofacial (**Figure 3**). However, due to the flexibility of the 11-membered ring and the signals overlap (e.g., H-1 and H-10), the relative configuration of other stereocenters (C-1, C-2, and C-10) on the ring could not be fully determined by ROESY spectrum. Thus, we performed theoretical NMR chemical shifts calculations of eight diastereomers (**Figure 4**) of **1** at mPW1PW91-SCRF/6-311G(d,p)//B3LYP-D3BJ/6-31G(d) theoretical level in methanol with the GIAO method (Wolinski et al., 1990). The calculated  $^{13}C$  and  $^1H$  NMR chemical shifts of (1*S*\*,2*S*\*,8*R*\*,9*S*\*,10*R*\*)-**1** showed the best agreement with the experimental values. Furthermore, DP4+ analysis (Grimblat et al., 2015) predicted that (1*S*\*,2*S*\*,8*R*\*,9*S*\*,10*R*\*)-**1** was the most likely candidates with 100% probability. The absolute configuration of **1** was assigned by the ECD calculation (**Figure 5**). The calculated ECD curve of (1*S*,2*S*,8*R*,9*S*,10*R*)-**1** matched well with the experimental curve, establishing the absolute configuration of **1** as 1*S*,2*S*,8*R*,9*S*,10*R*. Collectively, compound **1** was identified as shown in **Figure 1** and named penirolide A.

Compound **2** was isolated as yellow oil. Its molecular formula was determined as  $C_{17}H_{28}O_4$  from the positive ion at  $m/z$  319.1882  $[M + Na]^+$  (calcd for  $C_{17}H_{28}NaO_4$ , 319.1880) in the HRESIMS, corresponding to four degrees of unsaturation. The  $^1H$  NMR spectrum (**Table 1**) showed resonances for one olefinic proton ( $\delta_H$  5.61), three  $sp^3$  methines ( $\delta_H$  1.01, 2.93, and 3.04), five methyls ( $\delta_H$  0.87, 0.98, 1.15, 1.81, and 2.01), and three methylenes in which one methylene has exceptionally upfield chemical shifts ( $\delta_H$  0.53 and 0.38), suggesting the existence of a cyclopropane unit. The  $^{13}C$  NMR spectrum (**Table 1**) revealed the presence of 17 carbons comprising five methyls, three methylenes, five methines (including one olefinic and three oxygenated), and four non-protonated carbons (including one olefinic and one carbonyl). Three coupling spin systems, H-1–H-11 $\alpha$ /H-11 $\beta$ , H-3 $\alpha$ /H-3 $\beta$ –H-4–H-5, and H-7 $\alpha$ /H-7 $\beta$ –H-8, could be deduced from the  $^1H$ – $^1H$  COSY correlations (**Figure 2**). In the HMBC spectrum, correlations of  $\underline{CH}_3$ -12 ( $\delta_H$  0.87, s) with C-2 ( $\delta_C$  25.8), C-3 ( $\delta_C$  14.6), and C-4 ( $\delta_C$  24.5) indicated the presence of C-2–C-3–C-4 cyclopropane moiety, which connected with C-1 as established by the correlations from H-1 ( $\delta_H$  3.04) to C-2 and C-3. The HMBC correlations (**Figure 2**) from two methyls,  $\underline{CH}_3$ -13 ( $\delta_H$  1.15) and  $\underline{CH}_3$ -14 ( $\delta_H$  0.98), to C-5 ( $\delta_C$  72.7), C-6 ( $\delta_C$  39.4), and C-7 ( $\delta_C$  38.9), from H-5 ( $\delta_H$  2.93) to C-7 ( $\delta_C$  38.9), and from  $\underline{CH}_3$ -15 ( $\delta_H$  1.81) to C-8 ( $\delta_C$  126.8), C-9 ( $\delta_C$  132.2), and C-10 ( $\delta_C$  68.6) constructed a 10-membered ring with two geminal methyls at C-6 and one methyl at C-9, which fused with the above noted cyclopropane ring through C-2/C-3. Additional HMBC correlations from  $\underline{CH}_3$ -17 ( $\delta_H$  2.01) and H-10 ( $\delta_H$  5.61) to carbonyl C-16 ( $\delta_C$  170.3) enable attachment of an acetyl group to the C-10.

**TABLE 1** |  $^1\text{H}$  (500 MHz) and  $^{13}\text{C}$  NMR (125 MHz) data for compounds **1–3** ( $\delta$  in ppm,  $J$  in Hz).

No	<b>1<sup>a</sup></b>		<b>2<sup>b</sup></b>		<b>3<sup>b</sup></b>	
	$\delta_{\text{H}}$	$\delta_{\text{C}}$	$\delta_{\text{H}}$	$\delta_{\text{C}}$	$\delta_{\text{H}}$	$\delta_{\text{C}}$
1	3.43, t (7.7)	80.3, CH	3.04, dd (11.1, 4.5)	78.9, CH	2.71, dd (13.3, 3.0)	59.7, CH
2		75.6, C		25.8, C		59.6, C
3 $\alpha$	2.20, dd (14.0, 9.5)	45.6, CH <sub>2</sub>	0.53, dd (9.9, 4.4)	14.6, CH <sub>2</sub>	2.66, dd, (12.3,3.2)	42.9, CH <sub>2</sub>
3 $\beta$	2.28, dd (14.0, 4.4)		0.38, dd (5.7, 4.4)		0.63, dd (12.3, 10.5)	
4	5.47, ddd (15.8, 9.6, 4.3)	122.8, CH	1.01, dt (10.0, 5.7)	24.5, CH	2.76, ddd (10.2, 3.6, 2.4)	52.6, CH
5	5.43, dd (15.8, 1.1)	144.7, CH	2.93, d (6.1)	72.7, CH	2.33, d (2.4)	65.9, CH
6		36.1, C		39.4, C		34.4, C
7 $\alpha$	1.91, dd (13.7, 3.0)	45.1, CH <sub>2</sub>	1.76, ddd (14.6, 4.4, 2.3)	38.9, CH <sub>2</sub>	1.92, ddd (14.8, 4.3, 2.2)	38.7, CH <sub>2</sub>
7 $\beta$	1.27, dd (13.7, 11.4)		2.58, t (13.6)		2.62, m	
8	2.93 dd (11.4, 3.0)	63.7, CH	5.46, dd (12.6, 3.3)	126.8, CH	5.44, dd (12.5, 3.3)	127.7, CH
9		67.1, C		132.2, C		132.6, C
10	3.44, t (5.6)	75.6, CH	5.61, d (10.4)	68.6, CH	5.86, dd (12.0, 3.0)	68.7, CH
11 $\alpha$	2.01, dt (15.6, 1.6)	38.1, CH <sub>2</sub>	2.25, dt (14.0, 10.8)	36.4, CH <sub>2</sub>	1.78, m	31.1, CH <sub>2</sub>
11 $\beta$	1.22, ddd (15.6, 8.2, 5.9)		1.83, dd (14.0, 4.5)		2.26, dt (14.0, 3.0)	
12	1.08, s	22.3, CH <sub>3</sub>	0.87, s	12.6, CH <sub>3</sub>	1.27, s	18.2, CH <sub>3</sub>
13	1.06, s	28.5, CH <sub>3</sub>	0.98, s	21.9, CH <sub>3</sub>	1.12, s	29.7, CH <sub>3</sub>
14	1.11, s	26.7, CH <sub>3</sub>	1.15, s	25.9, CH <sub>3</sub>	0.77, s	17.9, CH <sub>3</sub>
15	1.24, s	16.5, CH <sub>3</sub>	1.81, brs	18.4, CH <sub>3</sub>	1.71, brs	18.7, CH <sub>3</sub>
16				170.3, C		170.1, C
17			2.01, s	21.5, CH <sub>3</sub>	2.05, s	21.3, CH <sub>3</sub>

<sup>a</sup>In MeOD.<sup>b</sup>In CDCl<sub>3</sub>.

The relative configuration of **2** was initially assigned by ROESY correlations. The ROESY correlations (**Figure 3**) of CH<sub>3</sub>-15 with H-8 ( $\delta_{\text{H}}$  5.46) and H-10 with H-7 $\alpha$  ( $\delta_{\text{H}}$  1.76)/H-7 $\beta$  ( $\delta_{\text{H}}$  2.58) indicated *Z* geometry for the  $\Delta^8$  double bond. The sequential ROESY correlations of H-10/H-4/H-1/H-3 $\beta$  placed

these protons on the same face the ring. The CH<sub>3</sub>-12 showed ROESY correlations with H-3 $\alpha$  and H-5, suggesting that they were located on the face opposite to H-4. However, relative configuration assignment only based on ROESY correlations is usually not reliable enough in conformationally flexible molecules

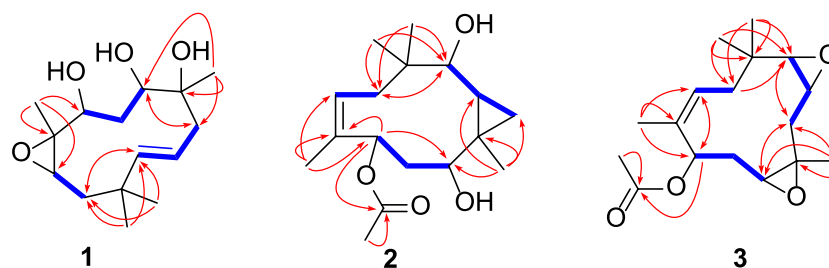


**FIGURE 2** | Key  $^1\text{H}$ - $^1\text{H}$  COSY (blue bold lines) and HMBC (red arrows) correlations of compounds **1-3**.

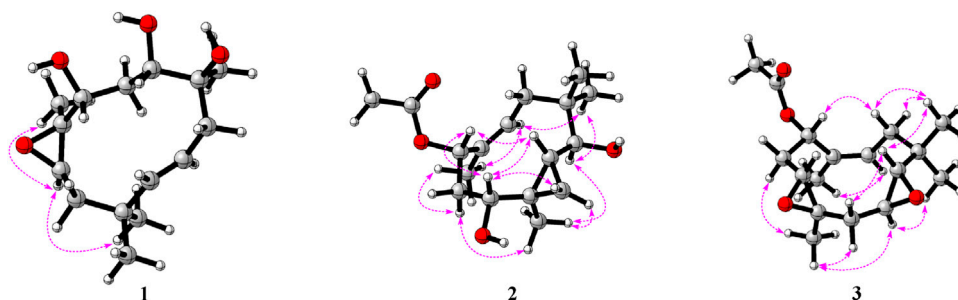


**FIGURE 3** | Key ROESY correlations of compounds **1-3**.

such as macrocycles. In order to irrefutably determine the relative configuration of the chiral centers (C-1, C-5, and C-10) on the macrocycle of **2**, eight possible diastereomers of **2** were applied to theoretical calculations of NMR chemical shifts followed by DP4+ analysis (**Figure 6**). The calculated chemical shifts of (1*R*\*,2*R*\*,4*R*\*,5*S*\*,10*S*\*)-**2** showed best agreement with the experimental values among the possible diastereomers and (1*R*\*,2*R*\*,4*R*\*,5*S*\*,10*S*\*)-**2** possessed 100% DP4+ probability (Grimblat et al., 2015), indicating that (1*R*\*,2*R*\*,4*R*\*,5*S*\*,10*S*\*)-**2** was the most likely candidate structure. The ECD calculation was further employed to clarify the absolute configuration of **2**. The calculated ECD curve of (1*R*,2*R*,4*R*,5*S*,10*S*)-**2** well fitted with the experimental one (**Figure 7**), defining the stereochemistry of **2** as 1*R*,2*R*,4*R*,5*S*,10*S*. Accordingly, compound **2** was elucidated as shown in **Figure 1** and named penirolide B.

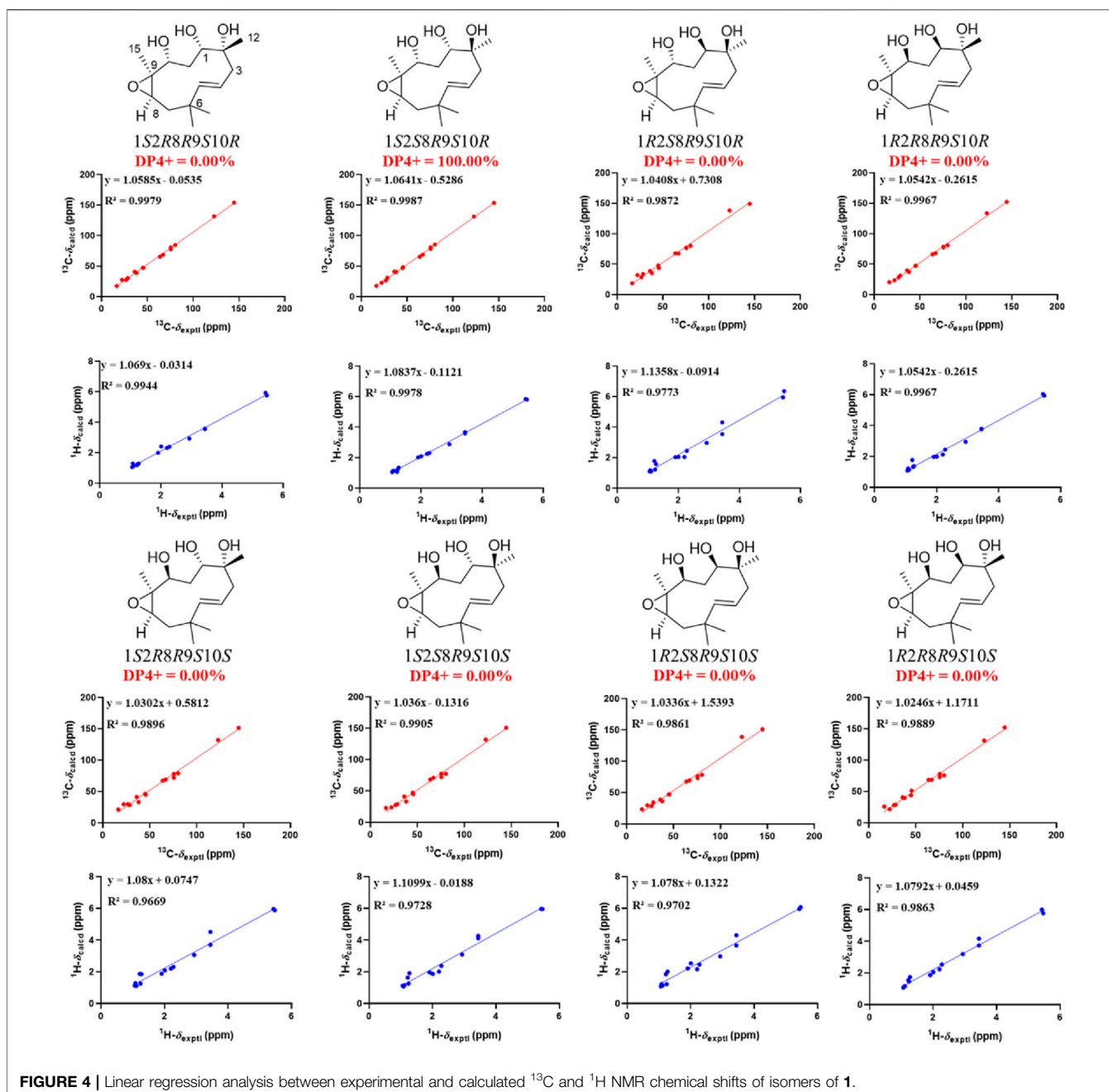
Compound **3** was obtained as yellow oil and its molecular formula of  $\text{C}_{17}\text{H}_{26}\text{O}_4$  was assigned by HRESIMS positive ion peak at 317.1723  $[\text{M} + \text{Na}]^+$  (calcd for  $\text{C}_{17}\text{H}_{26}\text{NaO}_4$ , 317.1723), indicating five degrees of unsaturation. The  $^1\text{H}$  NMR spectrum (**Table 1**) displayed signals for one olefinic proton ( $\delta_{\text{H}}$  5.44), four  $\text{sp}^3$  methines ( $\delta_{\text{H}}$  2.71, 2.76, 2.33, and 5.86), five methyls ( $\delta_{\text{H}}$  0.77, 1.12, 1.27, 1.71, and 2.05), and three methylenes. The  $^{13}\text{C}$  NMR spectrum (**Table 1**) showed resonances for 17 carbons ascribed by HSQC spectrum as five methyls, three methylenes, five methines (including one olefinic and three oxygenated), and four non-protonated carbons (including one olefinic and one carbonyl). These NMR data were very similar to that of phomanoxide (Zhang et al., 2015) whose structure was confirmed by

x-ray crystallography, with the only difference being the presence of an additional acetyl group [ $\delta_{\text{H}}$  2.05 (s, 3H),  $\delta_{\text{C}}$  21.3,  $\text{CH}_3$ -17;  $\delta_{\text{C}}$  170.1, C-16] in **3**. The deshielded shift of C-10 ( $\delta_{\text{C}}$  68.7;  $\Delta\delta_{\text{C}}$  2.1) in **3** relative to that of phomanoxide indicated that the acetyl attached at C-10, which was supported by the HMBC correlations from  $\text{CH}_3$ -17 and H-10 ( $\delta_{\text{H}}$  5.86) to carbonyl C-16 (**Figure 2**).

In the ROESY spectrum of **3**, the correlations of  $\text{CH}_3$ -12 with H-3 $\alpha$ , H-4, and H-11 $\alpha$  suggested that these protons resided on the same face of the molecule. Cross peak of H-3 $\beta$ /H-5 indicated that the two protons were cofacial (**Figure 3**). The large coupling constant  $J_{\text{H-10-H-11}\alpha} = 12.0$  Hz demonstrated that H-10 and H-11 $\alpha$  were *trans* oriented. Therefore, the relative configuration was proposed as 1*R*\*,2*R*\*,4*S*\*,5*S*\*,10*S*\*, which was further confirmed by the NMR chemical shift calculation (**Figure 8**) and its similar NMR data to that of phomanoxide. The 1*R*,2*R*,4*S*,5*S*,10*S* configuration for **3** was established based on its well-matched experimental and calculated ECD curves (**Figure 9**). Thus, the structure of **3** was elucidated as depicted in **Figure 1** and named 10-acetyl-phomanoxide.

In addition, three known compounds, aurasperone A (**4**) (Campos et al., 2005), pughinin A (**5**) (Pittayakhajonwut et al., 2002), and cyclo(L-Leu-L-Phe) (**6**) (Stark and Hofmann, 2005), were identified by comparison of their NMR data with literature data.

The liver plays a major role in whole body glucose metabolism by maintaining a balance between glucose production and glucose storage. Excessive hepatic glucose production contributes substantially to diabetes, and it is proposed that suppression of



hepatic glucose production may provide therapeutic advantages for the control of diabetes (Xiao et al., 2017; Liao et al., 2021). To investigate the anti-diabetic effect of the six compounds, we examined the glucose production in hepatocytes. Compounds **2**, **3**, **5**, and **6** significantly inhibited glucagon-induced hepatic glucose production, with  $\text{EC}_{50}$  values of 33.3, 36.1, 18.8, and 32.1  $\mu\text{M}$ , respectively, while it was  $>200 \mu\text{M}$  for Compounds **1** and **4**, and 2.3  $\mu\text{M}$  for the positive control metformin (Figure 10A). In response to glucagon, cAMP is a second messenger to initiate glucagon signaling cascades in hepatic glucose production. Compounds **2**, **3**, **5**, and **6** treatment suppressed cAMP accumulation (Figure 10B). These results indicated that

compounds **2**, **3**, **5**, and **6** inhibited hepatic glucose production by suppression glucagon-induced cAMP accumulation.

## MATERIALS AND METHODS

### General Experimental Procedures

Optical rotations were measured with a JASCO P-1020 digital polarimeter. The infrared spectra were recorded on a Shimadzu UV2550 spectrophotometer (Shimadzu, Kyoto, Japan). The mass spectrometric (HRESIMS) data were acquired using an API QSTAR Pulsar mass spectrometer (Bruker, Bremen, Germany).



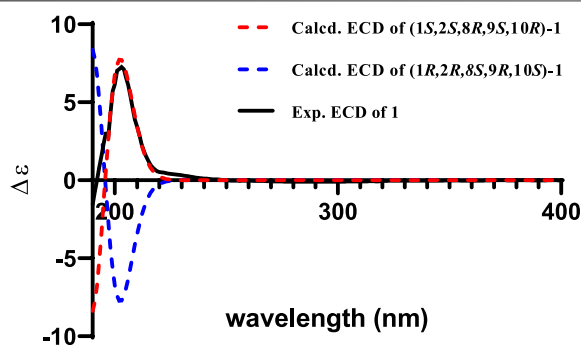


**FIGURE 5** | Experimental spectrum of **1** in methanol and calculated ECD spectra of (1S,2S,8R,9S,10R)-**1** and (1R,2R,8S,9R,10S)-**1**.

Semipreparative high-performance liquid chromatography (HPLC) equipped with octadecyl silane (ODS) column (Cosmosil ODS-A, 10 × 250 nm, 5 μm, 4 ml/min) was used to isolate compounds. The solvents used to the preparative HPLC, such as methanol, acetonitrile, hexane, and ethanol were of chromatographic grade (Concord Technology Co. Ltd., Tianjin, China). The solvents used to the extraction or isolation of the columns, such as ethyl acetate, methanol, chloroform, and methanol, were of analytical pure (Concord Technology Co. Ltd., Tianjin, China). The NMR spectra were recorded with a Bruker AV-500 spectrometer (Bruker, Bremen, Germany) using TMS as an internal standard. Silica gel (60–80 and 200–300 mesh; Qingdao Haiyang Chemical Co. Ltd., Qingdao, China) and Rp-C18 (20–45 μm; Fuji Silysia Chemical Ltd., Durham, NC, United States) were used for column chromatography.

### Fungal Material

The fungus *Penicillium* sp. was isolated from healthy papaya leaves collected in Haikou, Hainan Province, People's Republic of China, and identified by sequence analysis of the ITS region of rDNA (GenBank No. MT729953). A voucher strain was deposited in the Institute of Tropical Bioscience and Biotechnology.

### Fermentation and Isolation

Plugs of agar with mycelium were cut from solid medium and transferred aseptically to a 1,000-ml Erlenmeyer flask, containing 300 ml of liquid medium (glucose 10 g/L, maltose 20 g/L, monosodium glutamate 10 g/L, yeast extract 3 g/L, corn starch 1 g/L, mannitol 20 g/L, MgSO<sub>4</sub> 0.3 g/L, and KH<sub>2</sub>PO<sub>4</sub> 0.5 g/L). The whole culture broth (45 L) was harvested and filtered to yield the mycelium cake and liquid broth. The mycelium cake and liquid broth were extracted by EtOAc three times. The two EtOAc extracts were evaporated under reduced pressure and combined based on their similar metabolite profiles provided by HPLC analysis, affording a total of 12 g of EtOAc extract. The extract was separated by silica gel column eluted with different ratios of Petroleum ether-EtOAc (8:1, 6:1, 4:1, 2:1, 1:1, and 0:1) to afford six fractions (Fr.1–6). Fr.4 (0.52 g) was purified by a Rp-C<sub>18</sub> silica gel column (MeOH-H<sub>2</sub>O, 70%–30%), followed by semi-preparative HPLC (MeCN-H<sub>2</sub>O, containing 0.1% Formic acid, 50:50, v/v, 4.0 ml min<sup>-1</sup>) to obtain compounds **1** (7.0 mg, *t*<sub>R</sub>

= 9.5 min) and **2** (4.6 mg, *t*<sub>R</sub> = 6.5 min). Fr.3 (1.03 g) was applied to a Rp-C<sub>18</sub> silica gel column chromatography (MeOH-H<sub>2</sub>O, 50%–50%) and semi-preparative HPLC (MeCN-H<sub>2</sub>O, containing 0.1% Formic acid, 20:80, v/v, 4.0 ml min<sup>-1</sup>) to obtain compound **3** (4.8 mg, *t*<sub>R</sub> = 9.6 min). Fr.6 (1.01 g) was subjected to a Rp-C<sub>18</sub> silica gel column chromatography (MeOH-H<sub>2</sub>O, 80–20%) to obtain three subfractions (Fr.6.1–Fr.6.3). Compounds **4** (18.3 mg, *t*<sub>R</sub> = 8.3 min) and **5** (18.2 mg, *t*<sub>R</sub> = 7.5 min) were obtained from Fr.6.1 by semi-preparative HPLC (MeCN-H<sub>2</sub>O, containing 0.1% formic acid, 75:25, v/v, 4.0 ml min<sup>-1</sup>). Fr.6.3 (0.33 g) was subjected to semi-preparative HPLC (MeCN-H<sub>2</sub>O, containing 0.1% formic acid, 15:85, v/v, 4.0 ml min<sup>-1</sup>) to afford **6** (3.2 mg, *t*<sub>R</sub> = 10.5 min).

### Penirolide A (1)

Yellow oily; [α]<sub>D</sub><sup>25</sup> -9.0 (*c* 0.1, MeOH); UV (CH<sub>3</sub>OH) λ<sub>max</sub> (log $\epsilon$ ): 206 (2.52) nm; ECD (CH<sub>3</sub>OH) λ<sub>max</sub> (Δ $\epsilon$ ): 203 (7.25) nm; IR(KBr) ν<sub>max</sub>: 3,414, 2,962, 2,872, 1,727, 1,668, 1,453, 1,384, 1,285, 1,200, 1,091, 1,065, 990 cm<sup>-1</sup>; <sup>1</sup>H and <sup>13</sup>C NMR spectral data, **Table 1**; HRESIMS *m/z* 293.1723 ([M + Na]<sup>+</sup> (calcd for C<sub>15</sub>H<sub>26</sub>NaO<sub>4</sub>, 293.1723).

### Penirolide B (2)

Yellow oily; [α]<sub>D</sub><sup>25</sup> +3.0 (*c* 0.1, MeOH); UV (CH<sub>3</sub>OH) λ<sub>max</sub> (log $\epsilon$ ): 205 (2.56) nm; ECD (CH<sub>3</sub>OH) λ<sub>max</sub> (Δ $\epsilon$ ): 202 (8.09) nm; IR(KBr) ν<sub>max</sub>: 3,422, 2,960, 1,728, 1,453, 1,373, 1,248, 1,050, 960 cm<sup>-1</sup>; <sup>1</sup>H and <sup>13</sup>C NMR spectral data, **Table 1**; HRESIMS *m/z* 319.1882 [M + Na]<sup>+</sup> (calcd for C<sub>17</sub>H<sub>28</sub>NaO<sub>4</sub>, 319.1880).

### 10-Acetyl-phomanoxide (3)

Yellow oily; [α]<sub>D</sub><sup>25</sup> +31.9 (*c* 0.1, MeOH); UV (CH<sub>3</sub>OH) λ<sub>max</sub> (log $\epsilon$ ): 205 (2.55) nm; ECD (CH<sub>3</sub>OH) λ<sub>max</sub> (Δ $\epsilon$ ): 203 (10.12) nm; IR(KBr) ν<sub>max</sub>: 3,442, 2,961, 2,929, 1,736, 1,380, 1,242, 1,024 cm<sup>-1</sup>; <sup>1</sup>H and <sup>13</sup>C NMR spectral data, **Table 1**; HRESIMS *m/z* 317.1723 [M + Na]<sup>+</sup> (calcd for C<sub>17</sub>H<sub>26</sub>NaO<sub>4</sub>, 317.1723).

### NMR and ECD Calculations

The conformations of the isomers of compounds **1–3** were generated by iMTD-GC method embedded in Crest program (Pracht et al., 2020). Two conformations with the root-mean-square (RMS) distance and energy deviation of 0.5 Å and 0.25 kcal/mol, respectively, were considered as duplicates and one

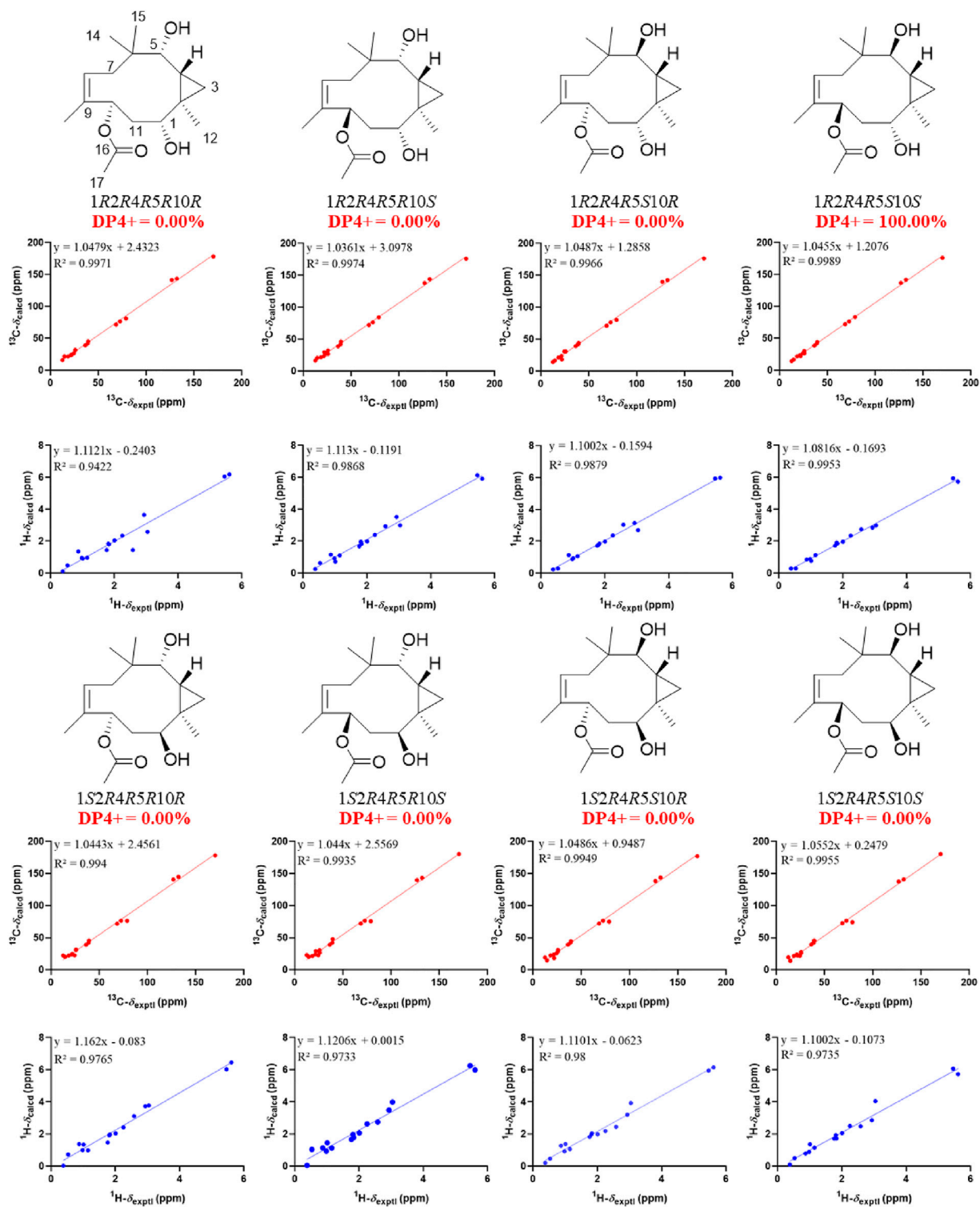
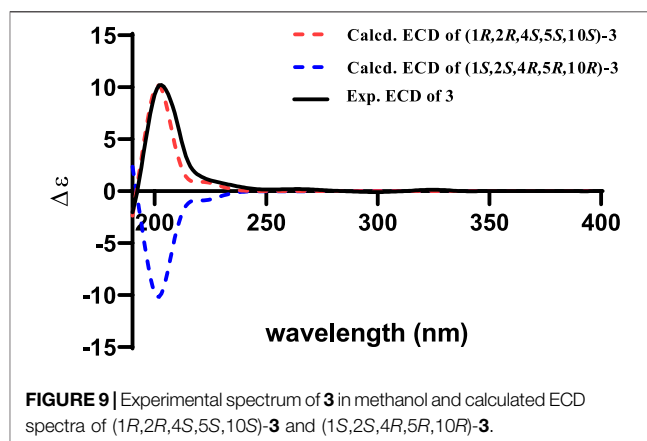
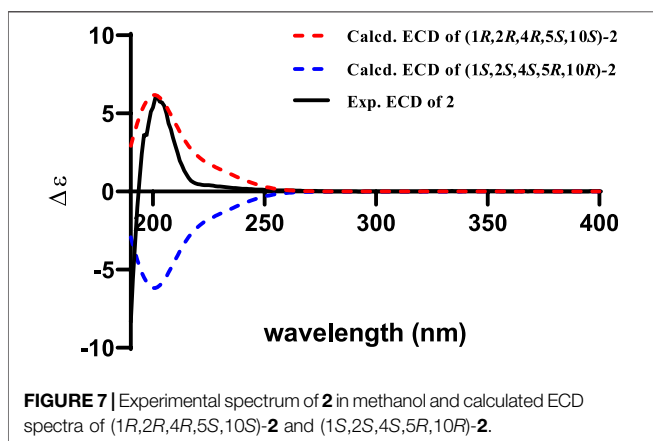


**FIGURE 6** | Linear regression analysis between experimental and calculated  $^{13}\text{C}$  and  $^1\text{H}$  NMR chemical shifts of isomers of **2**.

of them was removed. Density functional theory calculations were performed with the Gaussian 16 package (Frisch et al., 2019). The remaining conformers with population over 1% were optimized at

the B3LYP-D3BJ/6-31G(d) level in gas phase and the conformers within an energy window of 3 kcal/mol were kept. Then, these conformers were refined by re-optimizations at the B3LYP-D3BJ/6-

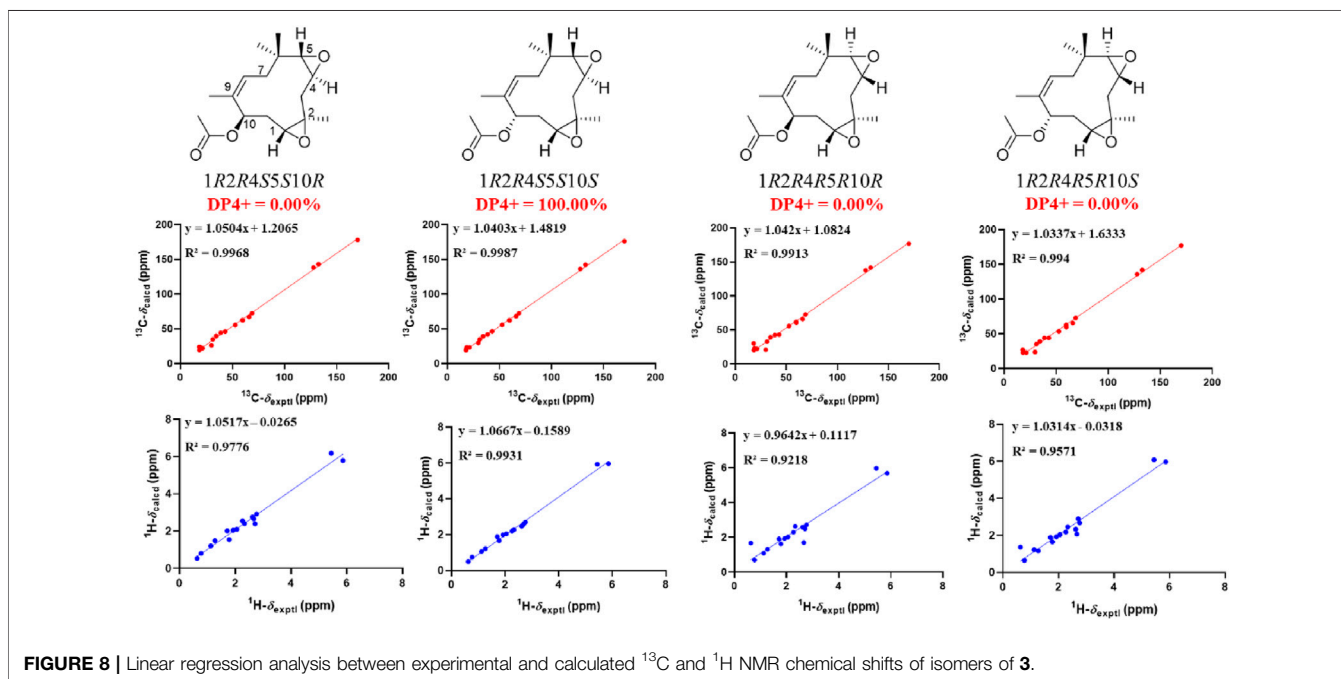


311G(d,p) level with the IEFPCM solvent model in methanol for **1** and chloroform for **2** and **3**, and frequency analysis of all optimized conformations was also performed at the same level of theory to ensure that no imaginary frequencies were present, confirming that the optimized structures were minima on their potential energy surfaces. NMR shielding tensors were calculated with the GIAO method (Wolinski et al., 1990) at the mPW1PW91/6-311G(d,p) level with the IEFPCM solvent model in methanol for **1** and chloroform for **2** and **3**. The calculated isotropic magnetic shielding constants ( $\sigma$ ) were Boltzmann averaged according to their Gibbs free energies. The shielding constants were converted into chemical shifts by referencing to TMS at 0 ppm according to the formula  $\delta_{\text{cal}} = \sigma_{\text{TMS}} - \sigma_{\text{cal}}$ , where the  $\sigma_{\text{TMS}}$  (the shielding constant of TMS) was calculated at the same level. For each candidate, the parameters  $a$  and  $b$  of the linear regression  $\delta_{\text{cal}} = a\delta_{\text{exp}} + b$ ; the correlation coefficient,  $R^2$ ; the mean absolute error (MAE) defined as  $\sum_n |\delta_{\text{cal}} - \delta_{\text{exp}}|/$

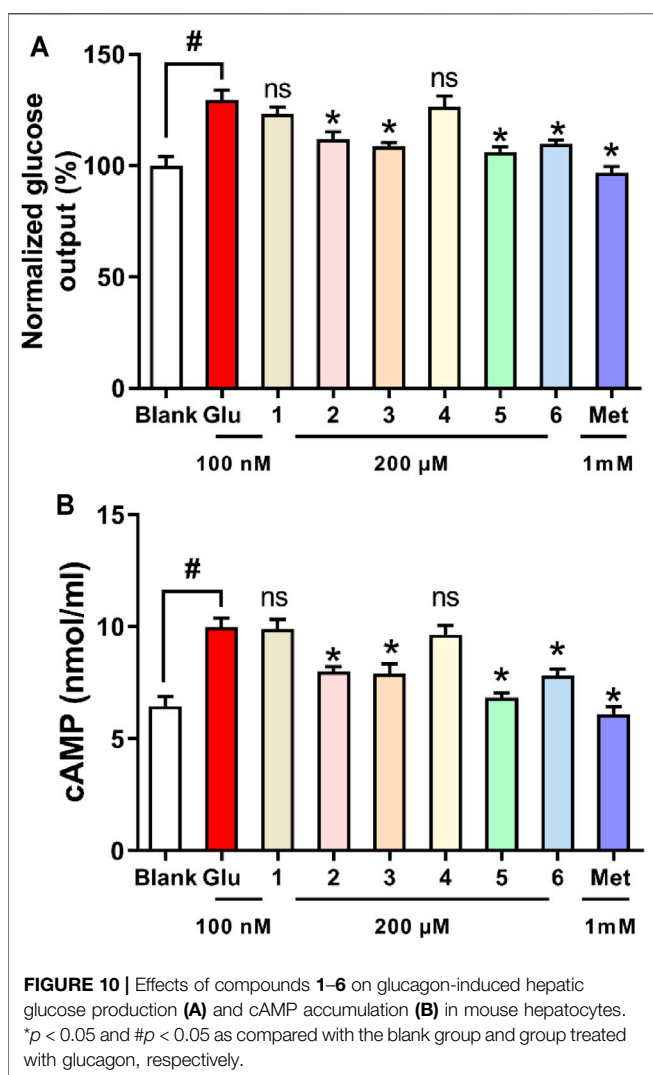
$n$ ; and the corrected mean absolute error, CMAE, defined as  $\sum_n |\delta_{\text{corr}} - \delta_{\text{exp}}|/n$ , where  $\delta_{\text{corr}} = (\delta_{\text{cal}} - b)/a$ , were calculated. DP4+ probability analysis was performed using the calculated NMR shielding tensors with DP4+ excel file (Grimblat et al., 2015). ECD spectra were calculated by the TDDFT methodology at the B3LYP/def2TZVP utilizing IEFPCM in methanol. The final ECD spectra were simulated by averaging the spectra of lowest energy conformers according to the Boltzmann distribution theory and their relative Gibbs free energy ( $\Delta G$ ) using SpecDis 1.71 (Bruhn et al., 2013) with  $\sigma = 0.30$  eV and uv shift = 5 nm for **1** and 10 nm for **2** and **3**, respectively.

## Primary Mouse Hepatocytes

Male C57BL/6J mice (6 weeks old) were purchased from Pengyue Laboratory Animal Company (Jinan, China). Animal care and experiments were approved by the Animal Ethics Committee of







Shandong Agriculture University. Primary mouse hepatocytes were prepared as previously described (Xiao et al., 2017). Briefly, fasted C57BL/6J male mice were anesthetized and livers were washed with Krebs-HEPES and digested with collagenase IV by perfusion through the inferior vena cava at 3 ml/min. Then, the whole liver was removed 6 min later, and hepatocytes were extracted in DMEM with 10% FBS. After filtering, cells were resuspended and cultured in 96- or 48-well plates. Then, the cells were treated as indicated.

### Measurement of Cell Viability and Glucose Production in Hepatocytes

Primary mouse hepatocytes were seeded in a 96-well plate and treated with 100 nM glucagon and various concentrations of test compounds (1–200  $\mu\text{M}$ ) for 24 h. After that, cell viability was assessed by the MTT method (Pan et al., 2021). For the

determination of glucose production, hepatocytes were incubated in KRB solution containing relevant substrates (10 mM pyruvate, 100 nM glucagon) or indicated compounds (1, 5, 10, 100, and 200  $\mu\text{M}$ ) for 6 h. Then, the cell supernatant was collected for glucose analysis using the commercial kit.

### Measurement of cAMP Production

Hepatocytes were incubated with the indicated compounds and stimulated with glucagon (100 nM) for 2 h, lysed in cell lysis buffer, and the supernatant was harvested for the assays of cAMP (Xiao et al., 2017). All data were expressed as the mean  $\pm$  SD from at least three independent experiments.

### DATA AVAILABILITY STATEMENT

The original contributions presented in the study are included in the article/Supplementary Material. Further inquiries can be directed to the corresponding authors.

### AUTHOR CONTRIBUTIONS

Y-XZ and PC contributed to the conception and design of the study. LY and F-DK determined the planar structures and absolute configurations, and wrote the draft of the manuscript. F-RW and Q-YM undertook the isolation and purification of all compounds. NX contributed to bioactivity assay. Q-YX undertook collection and identification of strain work. Y-GW and H-FD improved the manuscript. All authors contributed to manuscript revision as well as read and approved the submitted version.

### FUNDING

This research was supported by the Natural Science Foundation of Hainan Province (2019CXTD411), the Financial Fund of the Ministry of Agriculture and Rural Affairs, P. R. of China (NFZX2021), the Natural Science Foundation of Shandong Province (ZR2019BH080), the National Natural Science Foundation of China (82004014), the China Agriculture Research System (CARS-21), and the Central Public-Interest Scientific Institution Basal Research Fund for Chinese Academy of Tropical Agricultural Sciences (1630052017002 and 1630052021019).

### SUPPLEMENTARY MATERIAL

The Supplementary Material for this article can be found online at: <https://www.frontiersin.org/articles/10.3389/fchem.2021.797858/full#supplementary-material>

## REFERENCES

- Bruhn, T., Schaumlöffel, A., Hemberger, Y., and Bringmann, G. (2013). SpecDis: Quantifying the Comparison of Calculated and Experimental Electronic Circular Dichroism Spectra. *Chirality* 25, 243–249. doi:10.1002/chir.22138
- Campos, F. R., Barison, A., Daolio, C., Ferreira, A. G., and Rodrigues-Fo, E. (2005). Complete <sup>1</sup>H and <sup>13</sup>C NMR Assignments of Aurasperone A and Fonscinone A, Two Bis-Naphthopyrones Produced by *Aspergillus Aculeatus*. *Magn. Reson. Chem.* 43, 962–965. doi:10.1002/mrc.1654
- Frisch, M. J., Trucks, G. W., Schlegel, H. B., Scuseria, G. E., Robb, M. A., Cheeseman, J. R., et al. (2019). *Gaussian 16, Revision C.01*. Wallingford CT: Gaussian, Inc.
- Grimblat, N., and Sarotti, A. M. (2016). Computational Chemistry to the Rescue: Modern Toolboxes for the Assignment of Complex Molecules by GIAO NMR Calculations. *Chem. Eur. J.* 22, 12246–12261. doi:10.1002/chem.201601150
- Grimblat, N., Zanardi, M. M., and Sarotti, A. M. (2015). Beyond DP4: An Improved Probability for the Stereochemical Assignment of Isomeric Compounds Using Quantum Chemical Calculations of NMR Shifts. *J. Org. Chem.* 80, 12526–12534. doi:10.1021/acs.joc.5b02396
- Gupta, S., Chaturvedi, P., Kulkarni, M. G., and Van Staden, J. (2020). A Critical Review on Exploiting the Pharmaceutical Potential of Plant Endophytic Fungi. *Biotechnol. Adv.* 39, 107462. doi:10.1016/j.biotechadv.2019.107462
- Kaul, S., Gupta, S., Ahmed, M., and Dhar, M. K. (2012). Endophytic Fungi from Medicinal Plants: A Treasure Hunt for Bioactive Metabolites. *Phytochem. Rev.* 11, 487–505. doi:10.1007/s11101-012-9260-6
- Krishna, K. L., Paridhavi, M., and Patel, J. A. (2008). Review on Nutritional, Medicinal and Pharmacological Properties of Papaya (*Carica Papaya* Linn.). *Nat. Prod. Radianc* 7, 364–363.
- Liao, C.-S., Tang, C.-P., Yao, S., and Ye, Y. (2013). Humulane-type Sesquiterpenoids from *Pilea Cavalieriei* Subsp. *Crenata*. *Org. Biomol. Chem.* 11, 4840–4846. doi:10.1039/C3OB40872H
- Liao, W., Yang, W., Shen, Z., Ai, W., Pan, Q., Sun, Y., et al. (2021). Heme Oxygenase-1 Regulates Ferrous Iron and Foxo1 in Control of Hepatic Gluconeogenesis. *Diabetes* 70, 696–709. doi:10.2337/db20-0954
- Lodewyk, M. W., Siebert, M. R., and Tantillo, D. J. (2012). Computational Prediction of <sup>1</sup>H and <sup>13</sup>C Chemical Shifts: A Useful Tool for Natural Product, Mechanistic, and Synthetic Organic Chemistry. *Chem. Rev.* 112, 1839–1862. doi:10.1021/cr200106v
- Luo, D.-Q., Gao, Y., Gao, J. M., Wang, F., Yang, X. L., Liu, J. K., et al. (2006). Humulane-type Sesquiterpenoids from the Mushroom *Lactarius Mitissimus*. *J. Nat. Prod.* 69, 1354–1357. doi:10.1021/np060153l
- Pan, G., Zhao, Y., Ren, S., Liu, F., Xu, Q., Pan, W., et al. (2021). Indole-terpenoids with Anti-inflammatory Activities from *Penicillium* Sp. HFF16 Associated with the Rhizosphere Soil of *Cynanchum Bungei* Decne. *Front. Microbiol.* 12, 710364. doi:10.3389/fmicb.2021.710364
- Pinnamaneni, R. (2017). Nutritional and Medicinal Value of Papaya (*Carica Papaya* Linn.). *Wjpps* 6, 2559–2578. doi:10.20959/wjpps20178-9947
- Pittayakhajonwut, P., Theerasilp, M., Kongsaeer, P., Rungrod, A., Tanticharoen, M., and Thebtaranonth, Y. (2002). Pughinin A, a Sesquiterpene from the Fungus *Kionochaeta pughii* BCC 3878. *Planta Med.* 68, 1017–1019. doi:10.1055/s-2002-35653
- Pracht, P., Bohle, F., and Grimme, S. (2020). Automated Exploration of the Low-Energy Chemical Space with Fast Quantum Chemical Methods. *Phys. Chem. Chem. Phys.* 22, 7169–7192. doi:10.1039/C9CP06869D
- Smith, S. G., and Goodman, J. M. (2010). Assigning Stereochemistry to Single Diastereoisomers by GIAO NMR Calculation: The DP4 Probability. *J. Am. Chem. Soc.* 132, 12946–12959. doi:10.1021/ja105035r
- Smith, S. G., and Goodman, J. M. (2009). Assigning the Stereochemistry of Pairs of Diastereoisomers Using GIAO NMR Shift Calculation. *J. Org. Chem.* 74, 4597–4607. doi:10.1021/jo900408d
- Stark, T., and Hofmann, T. (2005). Structures, Sensory Activity, and Dose/Response Functions of 2,5-Diketopiperazines in Roasted Cocoa Nibs (*Theobroma Cacao*). *J. Agric. Food Chem.* 53, 7222–7231. doi:10.1021/jf051313m
- Strobel, G. A. (2003). Endophytes as Sources of Bioactive Products. *Microbes Infect.* 5, 535–544. doi:10.1016/S1286-4579(03)00073-X
- Toyota, M., Omatsu, I., Braggins, J., and Asakawa, Y. (2004). New Humulane-type Sesquiterpenes from the Liverworts *Tylimanthus Tenellus* and *Marchantia Emarginata* Subsp. *Tosana*. *Chem. Pharm. Bull.* 52, 481–484. doi:10.1248/cpb.52.481
- Uzma, F., Mohan, C. D., Hashem, A., Konappa, N. M., Rangappa, S., Kamath, P. V., et al. (2018). Endophytic Fungi-Alternative Sources of Cytotoxic Compounds: A Review. *Front. Pharmacol.* 9, 309. doi:10.3389/fphar.2018.00309
- Wolinski, K., Hinton, J. F., and Pulay, P. (1990). Efficient Implementation of the Gauge-independent Atomic Orbital Method for NMR Chemical Shift Calculations. *J. Am. Chem. Soc.* 112, 8251–8260. doi:10.1021/ja00179a005
- Xiao, N., Lou, M.-D., Lu, Y.-T., Yang, L.-L., Liu, Q., Liu, B., et al. (2017). Ginsenoside Rg5 Attenuates Hepatic Glucagon Response via Suppression of Succinate-Associated HIF-1 $\alpha$  Induction in HFD-Fed Mice. *Diabetologia* 60, 1084–1093. doi:10.1007/s00125-017-4238-y
- Zhang, H. W., Song, Y. C., and Tan, R. X. (2006). Biology and Chemistry of Endophytes. *Nat. Prod. Rep.* 23, 753–771. doi:10.1039/B609472B
- Zhang, J., Liu, L., Wang, B., Zhang, Y., Wang, L., Liu, X., et al. (2015). Phomanolides A and B from the Fungus *Phoma* sp.: Meroterpenoids Derived from a Putative Tropolonic Sesquiterpene via Hetero-Diels-Alder Reactions. *J. Nat. Prod.* 78, 3058–3066. doi:10.1021/acs.jnatprod.5b00969

**Conflict of Interest:** The authors declare that the research was conducted in the absence of any commercial or financial relationships that could be construed as a potential conflict of interest.

**Publisher's Note:** All claims expressed in this article are solely those of the authors and do not necessarily represent those of their affiliated organizations, or those of the publisher, the editors, and the reviewers. Any product that may be evaluated in this article, or claim that may be made by its manufacturer, is not guaranteed or endorsed by the publisher.

Copyright © 2021 Wang, Yang, Kong, Ma, Xie, Wu, Dai, Chen, Xiao and Zhao. This is an open-access article distributed under the terms of the Creative Commons Attribution License (CC BY). The use, distribution or reproduction in other forums is permitted, provided the original author(s) and the copyright owner(s) are credited and that the original publication in this journal is cited, in accordance with accepted academic practice. No use, distribution or reproduction is permitted which does not comply with these terms.